

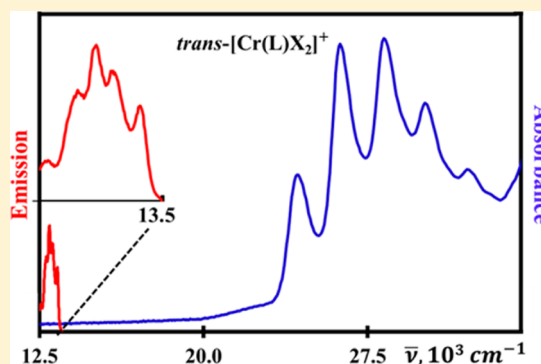
# To Be or Not To Be Symmetric: That Is the Question for Potentially Active Vibronic Modes

Sarah F. Tyler, Eileen C. Judkins, Dmitry Morozov, Carlos H. Borca, Lyudmila V. Slipchenko,<sup>id</sup> and David. R. McMillin\*<sup>id</sup>

Department of Chemistry, Purdue University, West Lafayette, Indiana 47906, United States

## S Supporting Information

**ABSTRACT:** Electronic spectra often exhibit vibronic structure when vibrational and electronic transitions occur in concert. Theory reveals (1) that orbital symmetry considerations determine specific roles played by the nuclear degrees of freedom and (2) that the vibrational excitation is often highly regiospecific, that is, attributable to an identifiable subset of atoms within the molecule. Spectra obtained from a chromium(III) complex involving a macrocyclic ligand and two axially disposed butadiynide groups nicely illustrate many of the concepts involved.



**KEYWORDS:** Upper-Division Undergraduate, Inorganic Chemistry, Spectroscopy, Coordination Compounds, UV–Vis Spectroscopy

Flame tests in the laboratory reveal that atoms frequently exhibit visible emissions,<sup>1,2</sup> but atoms have higher-energy electronic states as well. Molecular systems are even more complex. The major reason is the increased number of degrees of freedom because the wave functions of a molecule must account for the electrons of all atoms as well as the disposition of the nuclei. Fortunately, as outlined below, Born and Oppenheimer have shown that it is possible to treat the motions of electrons and nuclei separately because they move at such different speeds on average.<sup>3</sup> As a consequence, one can regard a molecule as a framework of atoms that has an equilibrium structure along with separate energy level schemes for rotational, vibrational, and electronic motion. Only the latter two types of motion persist in condensed phases since free rotation is not possible in such a collision-rich setting. Pure vibrational excitation proves to be a relatively low energy process that typically requires infrared energies. However, it is also possible to observe vibrational excitation in the visible or ultraviolet region of the electromagnetic spectrum, when it occurs in concert with electronic absorption or emission. Energy transfer between the radiation field and the molecule typically occurs via the electric dipole mechanism,<sup>4–6</sup> and a simultaneous vibrational and electronic, or vibronic, transition has energy  $\bar{\nu}_{el} \pm \bar{\nu}_{vib}$ , where  $\bar{\nu}_{el}$  and  $\bar{\nu}_{vib}$  designate the energies in wavenumbers of the participating electronic and vibrational transitions. Though ubiquitous, vibronic transitions traditionally receive little coverage in textbooks, to the point of omitting graphic illustrations.<sup>5,7</sup> Expanding the discussion along lines described below represents another approach that lends insight into vibronic processes, while underscoring foundational concepts of symmetry, bonding, and spectroscopy. A few

ground rules emerge that oftentimes foster a qualitative understanding of vibronic structure exhibited by a chromophore that may contain of many atoms.

The *trans*-[Cr(HMC)(C<sub>4</sub>H<sub>2</sub>)<sub>2</sub>]<sup>+</sup> complex (**1**), shown in Figure 1,<sup>8</sup> serves as an interesting example and is a focal point for the discussion to follow. A glance at the spectra provided in Figure 2 reveals the first take home lesson, which is that different vibrations couple to different electronic transitions. For example, the transitions in the low energy region between 12,500 and 13,500 cm<sup>-1</sup> in Figure 2 correspond to the low-temperature metal-centered, or d–d, emission spectrum of **1**. Here the spacing between adjacent vibronic peaks is variable but is always on the order of a couple hundred wavenumbers. In contrast, the absorption network centering around 27,500 cm<sup>-1</sup> exhibits a more regular vibronic spacing with an average peak-to-peak separation that is wider than the entire emission spectrum. Part of the explanation is that the electronically allowed absorption occurs in conjunction with particular vibrations that preserve the molecular symmetry, whereas the formally forbidden d–d emission depends on the participation of low-energy, symmetry-breaking vibrations, *vide infra*. As will also become clear, the active vibrations within each band system are regiospecific, that is, they logically relate to identifiable subsets of atoms within the molecule.

Received: April 29, 2017

Revised: June 29, 2017

Published: July 14, 2017

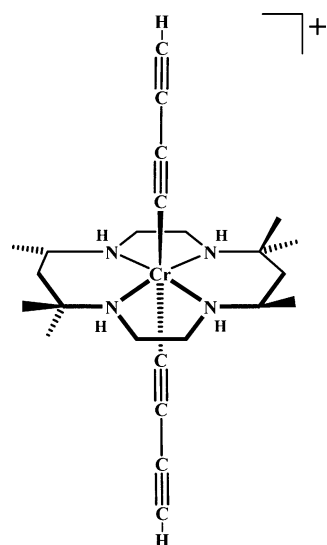


**Figure 1.** Complex 1, *trans*-dibutadiynido(*meso*-5,5,7,12,12,14-hexamethyl-1,4,8,11-tetraazacyclotetradecanyl)chromium(III) cation.

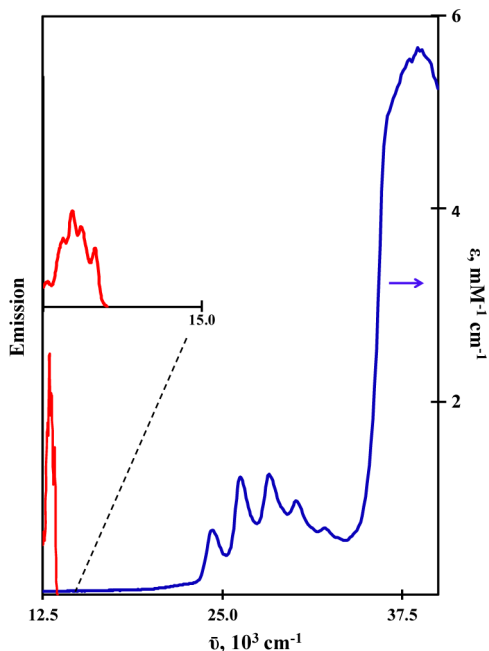


**Figure 2.** Absorption and emission spectra of 1. The absorbance spectrum (blue) is from a room-temperature solution in dichloromethane. The emission spectrum in red is from an alcohol glass at 77 K. Inset: Expanded energy range for emission from 12,500 to 15,000  $\text{cm}^{-1}$ .

## ■ BORN–OPPENHEIMER APPROXIMATION AND VIBRATIONAL COORDINATES

The theoretical treatment of vibronic transitions begins with the Born–Oppenheimer approximation.<sup>3,9,10</sup> The idea is that, because nuclei move at much slower speeds than electrons, one can solve Schrödinger's equation for the electronic degrees of freedom assuming that the nuclei are in specified positions. Calculating the energy as a function of the nuclear positions then defines a potential energy surface that governs nuclear motion and minimizes at the optimum nuclear arrangement. A nonlinear molecule containing  $N$  atoms has  $3N - 6$  degrees of vibrational freedom, and assuming the potential energy surface

is parabolic along each collective displacement, or normal coordinate, yields a ladder of vibrational energies as in Figure 3.

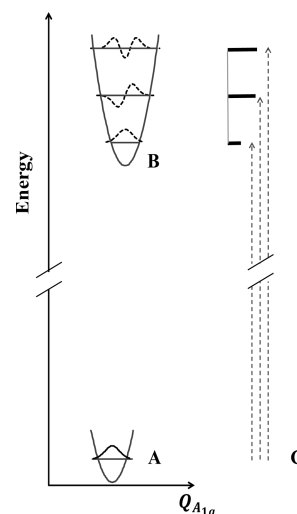


**Figure 3.** Vibronic energy levels and vibrational wave functions. (A) Potential energy function (gray) and ground state vibrational wave function  $\chi(0)$  (black) plotted along a totally symmetric normal coordinate, one of the  $3N - 6$  vibrational coordinates of the system. (B) The potential function of an excited electron electronic state and corresponding vibrational wave functions,  $\chi'(v_k)$  (dashed) for  $v_k = 0, 1$ , and 2. For simplicity, the plot assumes that the force constant is the same as in the ground state but there is a shift in equilibrium geometry. The data used to draw the ground-state curve pertain to the  $^{14}\text{N}^{16}\text{O}$  molecule, arbitrarily chosen for having a high frequency vibration. (C) Vibronic transitions to the three vibrational levels indicated in part B. Each relative intensity (horizontal bar length) is proportional to the square of the corresponding overlap integral,  $\langle \chi'(v_k) | \chi(0) \rangle$ , where  $v_k = 0, 1$ , or 2. Higher energy vibronic transitions not shown.

Equation 1 is a shorthand expression for the product wave function that describes the combined electronic and vibrational systems:

$$\psi_i \chi(v_1) \chi(v_2) \dots \chi(v_k) \quad (1)$$

where  $\psi_i = \psi_i(q, Q)$  denotes the wave function of the  $i$ th electronic state, with  $q$  and  $Q$  denoting the coordinates of all electrons and nuclei, respectively, and  $\chi(v_k)$  designates the vibrational wave function of the  $k$ th normal mode. The ground vibrational state for the  $k$ th normal mode has quantum number  $\nu_k = 0$ , and  $\nu_k$  increases by 1 for each successive vibrational level.

Multiple interactions help determine the equilibrium structure, to which one can assign a molecular point group that allows one to describe the associated vibrational wave functions in terms of their symmetry properties. In particular, the wave function for the ground vibrational state always forms a basis for the totally symmetric representation, and when  $\nu_k = 1$ , the wave function has the same symmetry as the normal coordinate,  $Q_k$ .<sup>5</sup> The normal coordinates of the system suffice to describe any change in the equilibrium geometry that may occur in an electronic excited state as well. However, nominally being a solution of the original Schrödinger equation, no isolated excited state is likely to adopt a new point group of its own accord.<sup>9–11</sup> The potential energy surface becomes more complex when two or more states that are degenerate or nearly degenerate experience Jahn–Teller coupling,<sup>12–15</sup> but such systems are beyond the purview of the present treatment. As

illustrated in Figure 3, however, expansion or contraction may occur along a totally symmetric vibrational coordinate that preserves the symmetry, especially when excitation alters the net number of bonding or antibonding electrons within the system.

### LIGAND TO METAL CHARGE TRANSFER ABSORPTION

The absorption band of **1** that centers around  $27,500\text{ cm}^{-1}$  is moderately intense with a maximum molar extinction coefficient of about  $1500\text{ M}^{-1}\text{ cm}^{-1}$  and is clearly spin-allowed. Neither the ligand nor the metal center exhibits an allowed absorption band in the visible region, so the absorption involves charge transfer from one moiety to another. In that Cr(II) is an easily formed oxidation state and the axial ligands are anionic and  $\pi$ -donating, one can confidently ascribe ligand-to-metal charge-transfer (LMCT) character to the absorption. Theoretical calculations for related systems are consistent with the proposed assignment.<sup>16</sup> One can further understand the excitation in terms of the energy-level diagram presented in Figure 4, which, for simplicity, assumes idealized  $D_{4h}$  symmetry.

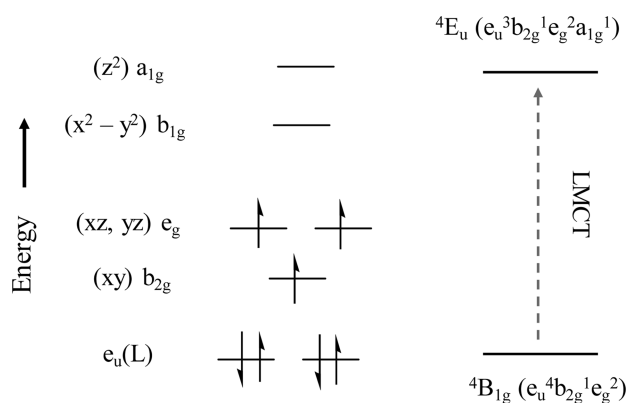


**Figure 4.** (left) Schematic orbital energy diagram showing the d-orbital splitting of **1** as well as largely ligand-based  $\pi$ -bonding orbitals of  $e_u$  symmetry. See the Supporting Information for related contour plots. (right) A state diagram showing terms involved in a LMCT transition. The Supporting Information also includes a discussion about deriving term labels.

In this view, interactions involving the four equatorial nitrogen and two axial carbon donor centers effectively determine the d-orbital splitting. Charge transfer could involve promotion of an electron into a  $d\sigma$  or a  $d\pi$  orbital; however, introducing another electron into one of the  $d\pi$  orbitals would require electron pairing, so injection of an electron into an empty  $d\sigma$  level is likely to be a lower energy process.<sup>17</sup> Whether to the  $a_{1g} d_{z^2}$  or  $b_{1g} d_{x^2-y^2}$  orbital, the excitation originates from one of two degenerate  $e_u(L)$  orbitals, which are C–C bonding. The excited state is therefore orbitally degenerate, and the full term symbol for the excited state is  ${}^4E_u$ . A standard correlation diagram reveals that  ${}^4B_{1g}$  is the term symbol for the ground state of a six-coordinate Cr(III) complex in  $D_{4h}$  symmetry, *vide infra*.

An allowed  ${}^4B_{1g} \rightarrow {}^4E_u$  LMCT transition must have a nonzero transition dipole moment, which implies that at least one integral of the following type is nonzero:

$$\langle \Psi_{E_u} | \hat{d} | \Psi_{B_{1g}} \rangle \quad (2)$$

where  $\Psi_{E_u}$  designates an excited state wave function,  $\hat{d}$  a dipole moment operator, and  $\Psi_{B_{1g}}$  the ground state wave function.<sup>5,6</sup>

Group theory reveals that the integral is nonzero if  $B_{1g} \otimes E_u \supset \Gamma_d$ , that is, the direct product of the symmetry species associated with the two wave functions includes at least one component of  $\Gamma_d$ , the representation or set of representations spanned by the dipole moment operators ( $x$ ,  $y$ , and  $z$ ). Here the  $E_u$  component, spanned by  $x$  and  $y$ , is the active part of  $\Gamma_d$ .

An allowed transition tends to exhibit vibronic structure when the excited state geometry shifts along one or more  $A_{1g}$  coordinates, as in Figure 3. A shift in geometry makes it possible for vertical jumps to occur from the  $\nu_k = 0$  level of the  ${}^4B_{1g}$  ground state to multiple vibrational levels of the  ${}^4E_u$  excited state. The transitions are “vertical” because there is no time for the nuclei to change positions during an electronic transition, in accordance with the Franck–Condon principle.<sup>10,18</sup> Vibrational overlap integrals dictate the relative peak heights, as illustrated in Figure 3C.<sup>19</sup> The clue to the nature of the vibrational excitation is that the spacing between peaks averages about  $1960\text{ cm}^{-1}$ , consistent with triple-bond stretching. As complex **1** has two C≡C stretching modes with  $A_{1g}$  symmetry, vibronic excitations involving each are theoretically possible, as are combination modes, etc. The details aside, what is important to note here is that the average C≡C stretching energy resolved in the absorption spectrum is less than the corresponding average ( $2106\text{ cm}^{-1}$ ) observed in the stretching region of the ground-state Raman spectrum. The obvious implication is that C≡C bond weakening occurs in the excited state, as one might expect to happen with the promotion of an electron out of a  $\pi$ -bonding level of the axial ligands. It also follows that the C≡C bonds will therefore lengthen in the excited state, the very type of displacement needed to explain the extended vibronic structure (Figure 3).

### METAL-CENTERED TRANSITIONS

A metal-centered, d–d transition is different by virtue of being an orbitally forbidden process in centrosymmetric environments. In such systems, a d–d transition involves a transition from one gerade (g) orbital to another, but the dipole moment operator is always ungerade (u). The direct products in eq 2 therefore have  $g \otimes u \otimes g = u$  symmetry, and the integrals necessarily vanish. As the d–d transitions are very weak and sometimes dwarfed by LMCT absorptions, the focus is on the well resolved d–d emission spectrum of **1**, measured at 77 K to enhance resolution. The lifetime of the emission signal is tens of microseconds, consistent with a spin-forbidden process. Formation of the emissive d–d excited state therefore involves inverting the spin of one of the  $d\pi$  electrons and decreasing the total spin quantum number from 3/2 to 1/2. A  ${}^2E_g$  state is, in fact, always the lowest energy doublet state in an octahedral Cr(III) complex, although a  ${}^2T_{1g}$  state occurs close by in energy.<sup>20</sup> However, in  $D_{4h}$  complexes like **1**, which has matched  $\pi$ -donating ligands in the axial positions, investigators usually ascribe the emission to a  ${}^2E_g$  state that derives from the  ${}^2T_{1g}$  state.<sup>21–24</sup> For more insight into the doublet states, see Supporting Information.

The very observation of an emission signal reveals, of course, that d–d transitions are at least partially orbitally allowed, thanks in good measure to vibronic effects.<sup>5,6</sup> The mechanism works by enabling an ostensibly forbidden transition to “steal” or borrow intensity from a neighboring allowed transition. For example, the  $E_g$  emitting excited state may take on some of the

character of the LMCT state with  $E_u$  symmetry discussed above. In order for the state mixing to occur, however, the molecule must first descend into a lower point group symmetry that lacks the center-of-inversion operation. Fortunately, low-symmetry excursions commonly occur, even in the vibrational ground state. Symmetry departures occur because quantum mechanics requires the system to retain zero-point vibrational energy so that the wave function distributes along *each* normal coordinate. In particular, consider the  $A_{2u}$  displacement, which destroys the center of inversion as the axial ligands become inequivalent (Figure 5).

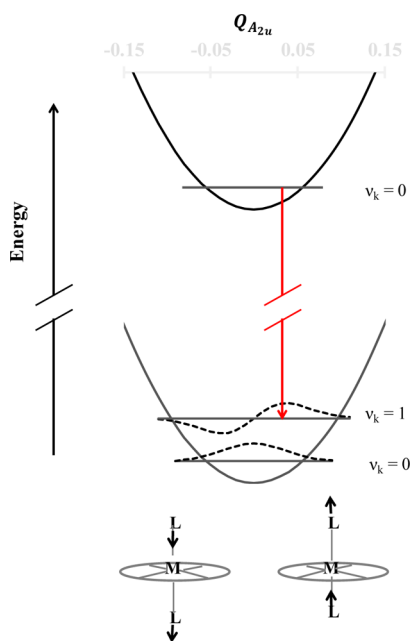


**Figure 5.** Schematic views of an  $A_{2u}$  vibration of **1** (bottom) and energy wells for the ground electronic and emissive d–d states (top). Note that in contrast to Figure 2, the two states share the same equilibrium geometry. In the time-average  $D_{4h}$  symmetry, the  $\nu_k = 0$  wave function of the d–d excited state is Gaussian, and the Franck–Condon factor is zero for a jump to the lower-energy  $\nu_k = 1$  level (red arrow). As explained in the text, however, the process becomes feasible during an excursion along the  $A_{2u}$  coordinate due to the  $Q_{A_{2u}}$  factor in the admixed wave function. Data used to plot the curves relate to  $^{63}\text{Cu}^{79}\text{Br}$  arbitrarily chosen for its metal–ligand stretching frequency.

Any time excursion along the  $A_{2u}$  coordinate occurs, the electronic degrees of freedom quickly respond, and perturbation theory reveals that the state does so by mixing with neighboring states. In the language of the original  $D_{4h}$  point group, the initial state takes on an admixture of the product wave function  $\Psi_{E_u} Q_{A_{2u}}$ , where functions  $\Psi_{E_u}$  and  $Q_{A_{2u}}$  denote the  $E_u$  electronic excited state and the normal coordinate associated with the  $A_{2u}$  promoting mode, respectively; see Supporting Information for more details. The  $Q_{A_{2u}}$  part of the admixture has two important consequences. First, it assures that the farther the distortion, the greater the  $\Psi_{E_u}$  character and the stronger the transition. Second, it modifies the Franck–Condon factor, and in that way continues the distortion by directing coexcitation of the  $A_{2u}$  promoting mode. In view of the large arrays of vibrations and electronic excited states available, many different vibronically allowed transitions are theoretically accessible. In theory, the  $E_g$  state may steal

intensity from any allowed  $\Psi_{\Gamma_u}$  state, with (ungerade)  $\Gamma_u$  symmetry, as long as the molecule has a normal coordinate with a symmetry matching one of those contained in the direct product  $\Gamma_u \otimes E_g$ .<sup>6,25</sup> A vibronic transition in the emission spectrum then has the energy  $\bar{\nu}_{el} - \bar{\nu}_{gr}$ , where  $\bar{\nu}_{el}$  denotes the energy of the pure electronic emission and  $\bar{\nu}_{gr}$  denotes the energy of the promoting mode.

In practice, however, only a limited number of the many possible transitions appear in the spectrum. For example, the emission spectrum in Figure 2 does not reveal a noticeable band shifted by anything like  $2100\text{ cm}^{-1}$ , even though complex **1** has a  $\text{C}\equiv\text{C}$  stretching vibration with  $A_{2u}$  symmetry. For a symmetry-breaking distortion to have real import, it must affect the makeup of molecular orbitals that are preponderantly 3d in character, because the emission remains essentially a metal-centered process. Thus, the effective modes are regiospecific and normally involve deformations of metal–ligand bonds. The latter vibrations tend to occur at relatively low energies due to bond strengths as well as the masses involved, but if mode assignments are available, one can attempt to identify the specific vibrations involved.<sup>24,26</sup> In addition to the promoting mode, the vibronically induced transition may result in the coexcitation of a totally symmetric vibration, as well as its harmonics. This possibility arises if the equilibrium structures of the initial and final electronic states occur at different positions along the latter coordinate. In principle, a sequence of transitions could emerge with Franck–Condon factors determining the relative intensities.

Due to the intensity borrowing mechanism, it may also be possible to observe non-totally symmetric modes within the vibronic envelope of a formally allowed electronic transition. However, such transitions are likely to be relatively weak and difficult to observe, except when the electronic transition itself is weak for some reason.<sup>27</sup> Finally, the energy and character of the enabling electronic state are always factors to consider. A LMCT state with  $B_{2u}$  symmetry could, for example, be quite capable of imparting intensity to the emission signal from **1**; see Supporting Information.

## ■ DOUBLET STATES OF CHROMIUM(III)

Before recapping, it is worth complementing the discussion with a brief look at some of the many d–d states actually available in chromium(III) systems. Figure 6 shows a ligand field theory model for the changes in state energies of a Cr(III) complex as the  $\pi$ -donating ability of the axial ligands increases and the symmetry descends from  $O_h$  to  $D_{4h}$ .<sup>22</sup> In  $O_h$  symmetry, the lowest energy  ${}^2E_g$  state entails a balanced occupation of all three degenerate  $d\pi$  orbitals, and no two electrons ever pair up in the same d orbital. However, in  $D_{4h}$  symmetry when  $\Delta E(\pi)$ , the energy splitting between the  $d\pi$  orbitals (Figure 4), is large, pairing two electrons in the lower energy  $b_{2g}$  orbital becomes favorable, and the  $b_{2g}^2 e_g^1$  configuration basically defines the emitting  ${}^2E_g$  state that derives from  ${}^2T_{1g}(O_h)$ .<sup>26</sup> At intermediate values of  $\Delta E(\pi)$ , however, electron–electron repulsions drive the  $d\pi$  electrons to spread into as many orbitals as possible,<sup>28</sup> and the  $e_g^3$  configuration also contributes to the makeup of the lowest energy  ${}^2E_g$  state. Indications are that **1** is also capable of emitting from a second thermally accessible doublet state, because higher energy components appear in the room-temperature emission spectrum.<sup>8</sup> Accordingly, the best guess is that the  $\Delta E(\pi)$  value of **1** falls near where multiple doublet states intersect in Figure 6, as indicated by the double arrow.

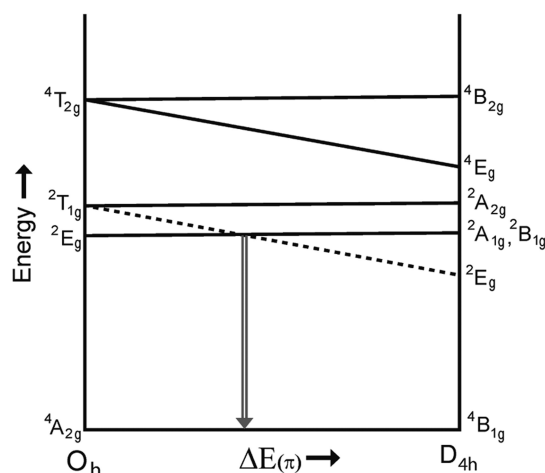


**Figure 6.** Metal-centered electronic states of Cr(III). The left-hand side of the diagram shows the states expected for a hypothetical octahedral ligand field. Moving from left to right the splitting between the  $e_g(xz, yz)$  and  $b_{2g}(xy)$  orbitals identified in Figure 4 grows due to the introduction of increasingly strong  $\pi$ -donating ligands in the axial positions. Adapted from ref 22. The double arrow indicates a  $\Delta E(\pi)$  value that could result in emission from more than one doublet state.

For a computational estimate of  $\Delta E(\pi)$ , it is convenient to downsize to the related  $d^1$  di(1,3-butadiynido) complex, *trans*-[Ti(NH<sub>3</sub>)<sub>4</sub>(C<sub>4</sub>H)<sub>2</sub>]<sup>+</sup> (2). Calculations show that its  $\Delta E(\pi)$  splitting has a respectable value of 2300 cm<sup>-1</sup>; see [Supporting Information](#) for details.

## OVERVIEW

Vibronic structure appears in absorption or emission bands when transitions occur to multiple vibrational levels of the final electronic state. Regiospecificity becomes apparent when the electronic reorganization involves orbitals that are specific to a locale or bond system within the molecule. In the case of an electronically *allowed* transition, the excited vibrations ordinarily correspond to totally symmetric modes or their harmonics. Contrarily, in the case of an orbitally *forbidden* transition, each vibronic component depends upon the participation of a fundamental mode that breaks the molecular symmetry. If the vibronic structure within a band is too extensive, it becomes unresolvable and effectively produces band broadening. In this regard, it is striking that such low energy vibrations are resolvable in the doublet-based emission spectra of Cr(III) complexes. Finally, mechanisms that can relax the spin selection rule or influence the polarizations of vibronic transitions are also important but beyond the scope of this short perspective.

## ASSOCIATED CONTENT

### Supporting Information

The Supporting Information is available on the ACS Publications website at DOI: [10.1021/acs.jchemed.7b00289](https://doi.org/10.1021/acs.jchemed.7b00289).

Development of  $\Psi_{E_g} Q_{A_{2u}}$  perturbation wave function, derivation of term symbols, intensity borrowing from a LMCT state with  $B_{2u}$  symmetry, and computational results for **2** including orbital contours of the metal-rich orbitals, a ball-and-stick drawing, predicted geometric properties, and methods used ([PDF](#))

## AUTHOR INFORMATION

### Corresponding Author

\*David R. McMillin. E-mail: [mcmillin@purdue.edu](mailto:mcmillin@purdue.edu).

### ORCID

Lyudmila V. Slipchenko: 0000-0002-0445-2990

David R. McMillin: 0000-0002-6025-0189

### Notes

The authors declare no competing financial interest.

## ACKNOWLEDGMENTS

D.M. gratefully acknowledges support from the Academy of Finland, while C.H.B. and L.V.S. acknowledge support of the National Science Foundation (Grant CHE-1465154). Information Technology at Purdue University provided computational resources. The authors are also grateful to reviewers and the editor for valuable suggestions.

## REFERENCES

- (1) Dragojlovic, V. Flame Tests Using Improvised Alcohol Burners. *J. Chem. Educ.* **1999**, *76*, 929–930.
- (2) Sanger, M. J.; Phelps, A. J. Simple Flame Test Techniques Using Cotton Swabs. *J. Chem. Educ.* **2004**, *81*, 969–970.
- (3) Born, M.; Oppenheimer, R. Quantum theory of molecules. *Ann. Phys.* **1927**, *389*, 457–484.
- (4) Drago, R. S. *Physical Methods for Chemists*, 2nd ed.; Saunders College Publishing: New York, 1992.
- (5) Douglas, B. E.; Hollingsworth, C. A. *Symmetry in Bonding and Spectra*; Academic Press, Inc.: New York, 1985.
- (6) McMillin, D. R. Electronic Absorption Spectroscopy. In *Physical Methods in Bioinorganic Chemistry*; Que, L., Jr., Ed.; University Science Books: Sausalito, CA, 2000; p 1–58.
- (7) Carter, R. L. *Molecular Symmetry and Group Theory*; John Wiley & Sons, Inc.: New York, 1998.
- (8) Tyler, S. F.; Judkins, E. C.; Song, Y.; Cao, F.; McMillin, D. R.; Fanwick, P. E.; Ren, T. Novel Cr(III)-HMC Alkynyl Complexes – Preparation and Emission Properties. *Inorg. Chem.* **2016**, *55*, 8736–8743.
- (9) Lee, S. Y. Potential Energy Surfaces and Effects on Electronic and Raman Spectra. *J. Chem. Educ.* **1985**, *62*, 561–566.
- (10) Sturge, M. D. The Jahn-Teller Effect in Solids. In *Solid State Physics*; Seitz, F.; Turnbull, D., Ehrenreich, H., Eds.; Academic Press: New York, 1967; Vol. 20, pp 178–186.
- (11) Pearson, R. G. *Symmetry Rules for Chemical Reactions*; Wiley-Interscience: New York, 1976; pp 474–478.
- (12) Bersuker, I. B.; Balabanov, N. B.; Pekker, D.; Boggs, J. E. Pseudo Jahn-Teller origin of instability of molecular high-symmetry configurations: Novel numerical method and results. *J. Chem. Phys.* **2002**, *117*, 10478–10486.
- (13) Pearson, R. G. Concerning Jahn-Teller Effects. *Proc. Natl. Acad. Sci. U. S. A.* **1975**, *72*, 2104–2106.
- (14) Wilson, R. B.; Solomon, E. I. Spectroscopic Studies of Photoactive  $^4T_{2g}$  Excited-State of HexammineChromium(III). *Inorg. Chem.* **1978**, *17*, 1729–1736.
- (15) Souissi, H.; Kammoun, S. Theoretical study of the electronic structure of a tetragonal chromium(III) complex. *J. Lumin.* **2011**, *131*, 2515–2520.
- (16) Berben, L. A.; Long, J. R. Homoleptic trimethylsilylacetylido complexes of chromium(III), iron(II), and cobalt(III): Syntheses, structures, and ligand field parameters. *Inorg. Chem.* **2005**, *44*, 8459–8468.
- (17) Klíxbüll Jørgensen, C. K. Electron Transfer Spectra. *Prog. Inorg. Chem.* **1970**, *12*, 101–158.
- (18) Flygare, W. H. *Molecular Structure and Dynamics*; Prentice-Hall, Inc.: Englewood Cliffs, NJ, 1978.

(19) Moomaw, W. R.; Skinner, J. F. Vibronic Spectra and Energy Levels of Polyatomic Molecules - Physical Chemistry Experiment. *J. Chem. Educ.* **1971**, *48*, 304–309.

(20) Flint, C. D.; Matthews, A. P.  $^4A_{2g} \leftrightarrow ^2E_g$  Transitions in *trans*-Cr(en)<sub>2</sub>Cl<sub>2</sub><sup>+</sup> and *trans*-Cr(tmd)<sub>2</sub>Cl<sub>2</sub><sup>+</sup>. *J. Chem. Soc., Faraday Trans. 2* **1980**, *76*, 1381–1387.

(21) Hoggard, P. E. Sharp Line Electronic Transitions and Metal-Ligand Angular Geometry. *Coord. Chem. Rev.* **1986**, *70*, 85–120.

(22) Forster, L. S. The Photophysics of Chromium(III) Complexes. *Chem. Rev.* **1990**, *90*, 331–353.

(23) Sun, C.; Turlington, C. R.; Thomas, W. W.; Wade, J. H.; Stout, W. M.; Grisenti, D. L.; Forrest, W. P.; VanDerveer, D. G.; Wagenknecht, P. S. Synthesis of *cis* and *trans* Bis-alkynyl Complexes of Cr(III) and Rh(III) Supported by a Tetradentate Macrocyclic Amine: A Spectroscopic Investigation of the M(III)-Alkynyl Interaction. *Inorg. Chem.* **2011**, *50*, 9354–9364.

(24) Lessard, R. B.; Heeg, M. J.; Buranda, T.; Perkovic, M. W.; Schwarz, C. L.; Yang, R. D.; Endicott, J. F. Stereochemical Alterations of <sup>2</sup>E Chromium(III) Excited-State Behavior in Dicyanotetraazacyclotetradecane Complexes - Ground-State X-ray Crystal Structures, Photophysical Behavior, and Molecular Mechanics Simulations of Stereochemical Effects. *Inorg. Chem.* **1992**, *31*, 3091–3103.

(25) Gouterman, M. Optical Spectra and Electronic Structure of Porphyrins and Related Rings. In *The Porphyrins*; Dolphin, D., Ed.; Academic Press: New York, 1978; Vol. III, Part A, pp 1–165.

(26) Flint, C. D.; Matthews, A. P.  $t_{2g}^3 - t_{2g}^3$  Transitions of the *trans*-Difluorobis(ethylenediamine)chromium(III) Ion - Vibronic Analyses and Crystal Field Calculations. *J. Chem. Soc., Faraday Trans. 2* **1974**, *70*, 1307–1315.

(27) Sponer, H.; Wollman, S. H. Analysis of the Near Ultraviolet Absorption Spectrum of Monochlorobenzene. *J. Chem. Phys.* **1941**, *9*, 816–825.

(28) McMillin, D. R. When One Configuration Is Not Enough. *J. Chem. Educ.* **2008**, *85*, 859–862.